Optical Materials 126 (2022) 112197

Contents lists available at ScienceDirect

Optical Materials

journal homepage: www.elsevier.com/locate/optmat

Femtosecond-laser fabrication of magneto-optical waveguides in terbium doped CaLiBO glass

S.N.C. Santos [a], A.L.S. Romero [a], B.C. Menezes [a], R.Q. Garcia [a], J.M.P. Almeida [a,b], A. C. Hernandes [a], L. De Boni [a], C.R. Mendonca [a,*]

[a] University of São Paulo, São Carlos Institute of Physics, 13560-970, São Carlos, SP, Brazil
[b] Federal University of São Carlos, Physics Department, 13565-905, São Carlos, SP, Brazil

ARTICLE INFO

Keywords:
Femtosecond laser micromachining
Glass waveguides
CaLiBO glass
Faraday effect
Verdet constant
Rare-earths

ABSTRACT

Femtosecond laser micromachining has potential application in integrated photonics thanks to its ability to produce micrometer-size three-dimensional structures in different types of materials, including the ones whose properties can be externally altered, which allows for the fabrication of optically active devices. In this work, we demonstrate the fs-laser fabrication of magneto-optical waveguides in CaLiBO (calcium-lithium tetraborate) glasses codoped with Yb^{+3} and Tb^{3+} ions. Single-mode type waveguides were produced using fs-pulses with ~0.1 J/cm^2 and 6.5×10^5 pulses/spot, an important feature for integrated photonic devices. The fabricated waveguides display Faraday effect, with a Verdet constant of $560^\circ\ T^{-1}m^{-1}$, for the sample containing 2% of Tb^{3+}, which is equivalent to the one observed for the bulk. Such a result demonstrates that fs-laser micromachining, in the conditions used here, does not negatively affect the magneto-optical properties of the sample. Thus, our results open a new pathway towards the processing of magneto-optical waveguides aimed at applications in magneto-optical photonic microdevices.

1. Introduction

Waveguides are a fundamental part of integrated photonics, not only for connecting distinct components in devices but also as active elements that can alter light's properties. Femtosecond laser microfabrication is a simple, non-contact, single-step technique widely used for fabricating a myriad of components, such as splitters, interferometers, resonators, and particularly waveguides [1–3]. Thanks to the nonlinear nature of the light-mater interaction when ultrashort pulses are used, energy transfer to the material is confined to the focal volume, which makes this technique an effective tool for processing materials with precision and high spatial resolution [4]. Hence, fs-laser micromachining has been applied, for instance, in fluidic optical waveguides [5], sensors [6], generation of nanoparticles [7], control wettability [8], etc.

The interest in employing fs-laser micromachining to fabricate optically active waveguides has been growing in the last few years with the demonstration, for example, of emissive ones [9,10]. Materials exhibiting the Faraday effect, which corresponds to a rotation of the light-polarization by an externally applied magnetic field, can be combined with fs-laser micromachining to obtain optically active waveguides, as demonstrated in Refs. [11–15]. In this direction, magneto-optic glasses have appeared as an interesting class of materials for photonics [16]. Such glasses present Faraday effect, which is characterized by the Verdet constant (V). The higher V, the larger the rotation of light polarization induced by the magnetic field for a given material length over which the interaction occurs. Materials exhibiting Faraday effect usually contain high concentrations of rare-earth ions in their composition [17]. Among the rare-earth ions, Tb^{3+} is the most used element and provides a high Verdet constant [18]. For example, Terbium Gallium garnet (TGG) is a magneto-optical material that has been widely used in optical insulators [19] and magneto-optical switching [20]. Likewise, magneto-optical glasses, for example, have been used as Faraday rotators [21] and optical isolators [22], which are essential components for polarization control and birefringence compensation [23].

Here we demonstrate the fabrication of waveguides by femtosecond laser micromachining in CaLiBO (calcium-lithium tetraborate) glasses doped with Tb^{3+} and Yb^{3+}. Such glass matrix have already been reported as a down-converter for solar cells [24], fluorescent waveguides [10], and nonlinear optical material [25]. We found the optimum

* Corresponding author.
E-mail address: crmendon@ifsc.usp.br (C.R. Mendonca).

https://doi.org/10.1016/j.optmat.2022.112197
Received 27 January 2022; Received in revised form 3 March 2022; Accepted 4 March 2022
Available online 7 March 2022
0925-3467/

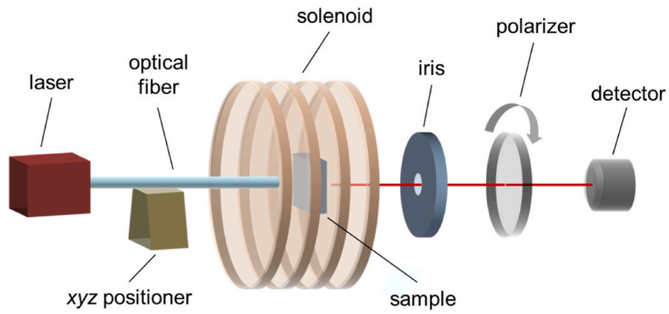

Fig. 1. Experimental setup for the Faraday rotation measurements.

conditions for waveguides fabrication based on their homogeneity, mode profile, and losses. The produced waveguides display Faraday effect, with Verdet constants of −290 and −561° $T^{-1}m^{-1}$ for CaLiBO samples with 1% and 2% of Tb^{3+}, respectively, which is equivalent to the one observed for the bulk material.

2. Experimental

The CaLiBO matrix were fabricated by the melt-quenching technique, as described in Ref. [25], and contain $60B_2O_3 + 30CaO + 10Li_2O$ (mol%). The samples used in the work are codoped with Tb^{3+} and Yb^{3+}, with composition (99% - x) CaLiBO + 1% Yb_2O_3 + x% Tb_4O_7 with x = 1.0 and 2.0 (mol%); such samples are designated as CaLiBO1 and CaLiBO2, respectively.

Waveguides were micromachined using a Ti:sapphire laser oscillator at 800 nm, with a maximum energy of 100 nJ, operating at 5 MHz repetition rate and delivering 50-fs pulses [26]. The laser beam was focused by a 0.65-NA microscope objective in the sample, that is translated in a *xyz* stage moved a constant speed. The guiding characteristics of the fabricated waveguides, specifically the waveguide losses, guided mode profile and induced refractive index change, were measured using an objective lens to couple light from a HeNe laser (632.8 nm). In this coupling system, an objective lens (NA = 0.40) focuses the laser beam in the waveguide input. The light transmitted through the waveguide is collected by an output objective lens (NA = 0.25). More details of the coupling system can be seen in Ref. [26]. Total losses are calculated by measuring the input and the output power, including the transmission of the optical components of the system. With the aid of a CCD camera, the guided modes of the fabricated waveguides are measured. The coupling losses are estimated, determining the mode mismatch between the profiles of the guided mode and the input laser beam, according to the method described in Refs. [27,28]. Thus, guiding loss is determined by subtracting the coupling loss from the total losses.

The produced waveguides were also characterized by bright-field optical microscopy using a Zeiss optical microscope model LSM 700 coupled to a CCD camera, which allowed evaluating the cross-section and the top view of the waveguides.

The measurement of the Verdet constant was performed in the bulk sample and the waveguides using the polarization rotation configuration, shown schematically in Fig. 1. The sample is positioned in the center of a solenoid, in order to achieve a uniform magnetic field across its length. A He–Ne laser (632.8 nm) is coupled to a polarization-maintaining fiber, which is mounted in a *xyz* positioning stage used to align the light in the case of the waveguide; for the bulk sample such fine alignment is not necessary. An iris is placed after the solenoid to delimit the guided light and block any scattered light. The polarization rotation is determined using a rotating polarizer (analyzer) positioned before the detector, with the aid of a lock-in amplifier referenced by a signal generated from the rotating analyzer driver.

Laser Induced Breakdown Spectroscopy (LIBS) was used to obtain the stoichiometry of the sample beyond the nominal value for the concentrations. LIBS was performed in a homemade setup that uses a 150-fs pulses from a Ti:sapphire laser amplifier (CLARK MXR-2001) centered at 775 nm with a 1 kHz repetition rate. The laser beam is focused on the sample to a spot of ~17 μm and maximum pulse energy at the sample of 390 μJ was employed. The generated plasma spectrum is collected and analyzed in a spectrometer with 0.75 μm FWHM optical resolution.

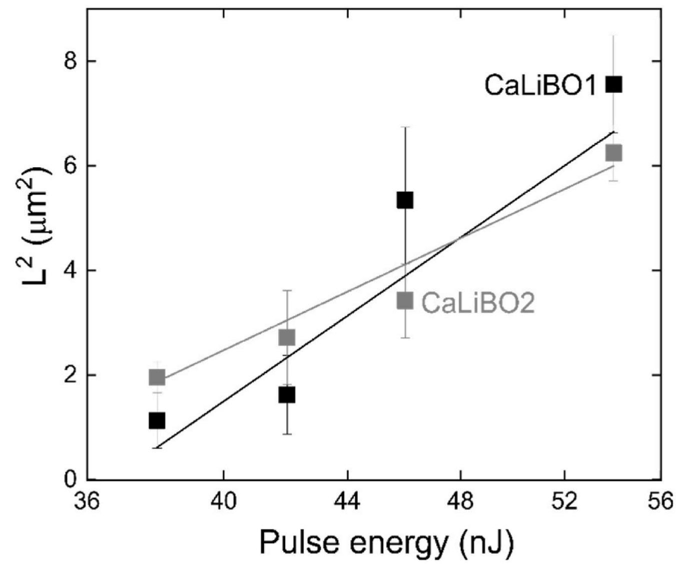

Fig. 2. Squared line (L^2) as a function of the pulse energy (log scale) for CaLiBO1 and CaLiBO2 at scanning speeds 50 μm/s.

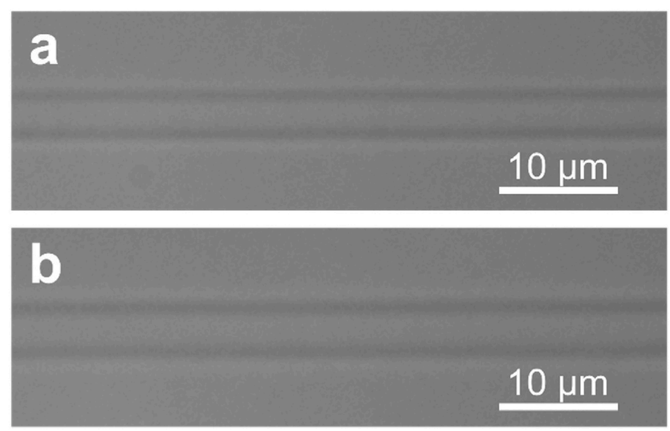

Fig. 3. Optical microscopy of the top view of the waveguides in (a) CaLiBO1 and (b) CaLiBO2.

3. Results

LIBS was carried out to investigate the stoichiometry of samples CaLiBO1, CaLiBO2, and CaLiBO (glass matrix without rare-earths dopants) as reference. The LIBS spectra contain all the main Ca and Li lines. For the doped samples, it was possible to observe the emissions from Yb and Tb, whose total areas were considered to quantify the presence of Tb and Yb (results not shown). The spectra used a normalization by the total plasma emission intensity, as described in Ref. [29]. Our results reveal that the ratio of the Tb concentration between CaLiBO2 and CaLiBO1 is (1.9 ± 0.2), which is very close to the nominal one.

Fig. 2 shows the influence of the fs-pulse energy on the half-line width squared (r^2) as a function of the pulse energy (log–scale), of lines micromachined in the volume of the samples, for a scanning speed of 50 μm/s that corresponds to approximately 6.5 × 10^5 pulses/spot. The lines-widths ($2r$) values, for both samples, increase with pulse

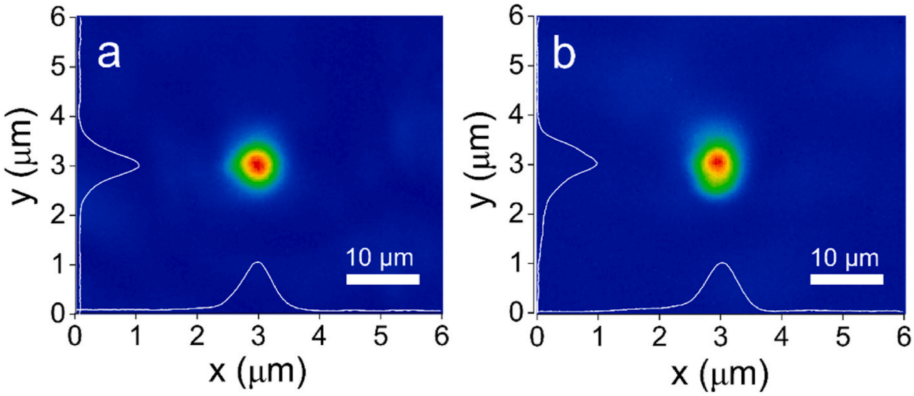

Fig. 4. Image of propagated modes at 632.8 nm for (a) CaliBO1 and (b) CaLiBO2 and their respective vertical and transverse profiles.

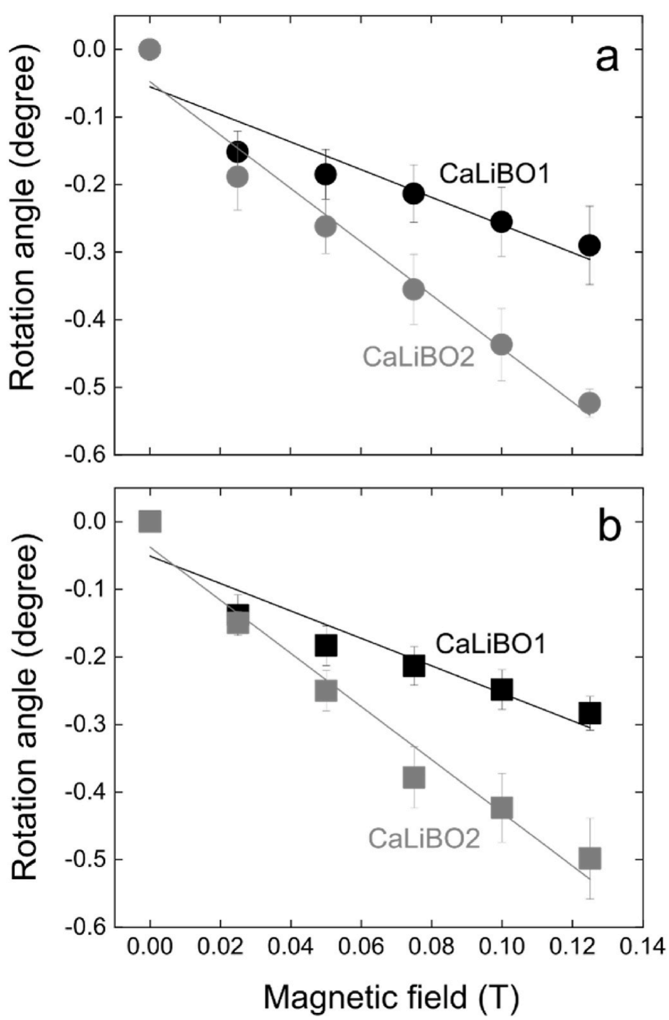

Fig. 5. Faraday rotation angle versus the magnetic field (a) CaLiBO bulk and (b) CaLiBO waveguide glasses.

fluence, varying from approximately 2.2 to 4.6 μm when the pulse energy increases from 38 to 54 nJ. The linear behavior observed Fig. 2 reveals that the micromachined regions follow the laser beam Gaussian profile. By fitting the data shown in Fig. 2 using the model proposed in Ref. [30], we determined the threshold energies (F_{th}), which are 0.07 and 0.09 J/cm^2 for CaLiBO1 and CaLiBO2, respectively. Such values represent the minimum fluence that needs to be used to modify the sample.

Table 1
Values of Verdet constants for CaLiBO1 and CaLiBO2.

Sample glasses	% codoping		Verdet constant (°T^{-1}m^{-1})	
	Yb^{3+}	Tb^{3+}	Bulk	Waveguides
CaLiBO1	1%	1%	−292 ± 5	−290 ± 20
CaLiBO2	1%	2%	−560 ± 40	−561 ± 5

Fig. 3 shows optical microscopy images of the longitudinal (top) view of waveguides produced by fs-laser micromachining in CaLiBO1 and CaLiBO2 samples. These structures were produced using a fluence of 0.1 and 0.15 J/cm^2 (~6.5 × 10^5 pulses/spot), which were determined as the best conditions to achieve homogeneous waveguides. Such waveguides were inscribed at approximately 100 μm below the sample surface to avoid spherical aberration and self-focusing, and with a total length of 7 mm.

The mode profile of guided light at 632.8 nm shown in Fig. 4 demonstrates that the fabricated waveguides support the single-mode type operation, with an almost Gaussian intensity distribution, as displayed by the x and y profiles in Fig. 4. Assuming the fabricated waveguides can be described by step-index waveguides (cylindrical inner core of refractive index n surrounded by an external cladding of slightly lower refractive index, which in our case is the refractive index of the glass). One is able to fit the measured output mode profile (similar to the ones displayed in Fig. 4) with the well-known solution for the light distribution, i.e., a Bessel function of the first kind for the core and a Bessel function of the second kind for the cladding [31]. With such an approach, we estimated the laser-induced refractive index change as being of the order of 10^{-4}, which corresponds to a numerical aperture of about 0.08.

The total losses of the waveguides were determined by measuring the light transmittance (632.8 nm) using an objective lens-based coupling system, taking into account the input and output objectives transmission (95% and 97%, respectively). Coupling losses were estimated by considering the Fresnel reflection and calculating the mode mismatch loss (~3.6 dB) [27,28]. By subtracting the total losses from the coupling losses, one determined a guiding loss of ~ (0.2 ± 0.1) dB/mm for both samples.

Fig. 5 shows the rotation angle as a function of the magnetic field for bulk (a) and fabricated waveguides (b) for both samples. The Verdet constant is obtained from the slope of linear fit (solid lines in Fig. 5). For the bulk CaLiBO1 and CaLiBO2 samples, the average values of the Verdet constant are displayed in Table 1. Therefore, the Verdet constants for bulk and waveguides are the same, within the experimental error, indicating that fs-laser microfabrication does not impair the magneto-optical effect of CaLiBO glasses. As mentioned before, the Verdet constant describes the magnitude of the magneto-optical effect, and it is directly proportional to the content of Tb^{+3} ions in the sample. Thus, the

Faraday effect for CaLiBO2, which has 2%mol of the Tb^{3+}, should be twice higher than that for CaLiBO1, as observed in Table 1. Waveguides fabricated by fs-laser in a commercial Faraday glass (TG20) have shown a slight decrease in the Verdet constant compared to that of the bulk glass [12].

It is worth noting that the Verdet constant increases by a factor of 1.9 for CaLiBO2 in comparison to CaLiBO1. Such factor matches precisely the proportion of Tb concentration between the samples, determined by LIBS, since terbium ions are responsible for the Faraday effect [11,24].

4. Conclusions

We demonstrated the fabrication of waveguides, by fs-laser micromachining, in CaLiBO glasses codoped with Yb^{3+} and Tb^{+3}, which exhibit the Faraday effect. After determining the ideal experimental conditions, homogeneous waveguides were produced using fs pulses with a fluence of ~0.1 J/cm^2 (6.5 × 10^5 pulses/point). Such waveguides exhibit single-mode type operation and display the magneto-optical effect, as its bulk counterpart. Since the Verdet constants of the waveguides are equivalent to the one for the bulk, fs-laser micromachining does not impair the magneto-optical response of the sample in the fabrication conditions proposed here. Therefore, our results pave the way for processing magneto-optical waveguides aimed at applications in magneto-optical integrated photonics.

CRediT authorship contribution statement

S.N.C. Santos: Conceptualization, Methodology, Investigation, Writing – original draft, Writing – review & editing. **A.L.S. Romero:** Conceptualization, Methodology, Investigation, Writing – review & editing. **B.C. Menezes:** Conceptualization, Methodology, Investigation, Writing – review & editing. **R.Q. Garcia:** Conceptualization, Methodology, Investigation, Writing – review & editing. **J.M.P. Almeida:** Methodology, Resources, Writing – review & editing. **A.C. Hernandes:** Resources, Writing – review & editing. **L. De Boni:** Conceptualization, Methodology, Validation, Investigation, Writing – review & editing. **C. R. Mendonca:** Conceptualization, Methodology, Validation, Investigation, Writing – original draft, Resources, Writing – review & editing, Visualization, Supervision, Project administration, Funding acquisition.

Declaration of competing interest

The authors declare that they have no known competing financial interests or personal relationships that could have appeared to influence the work reported in this paper.

Acknowledgments

The authors gratefully acknowledge financial support from the Coordenação de Aperfeiçoamento de Pessoal de Nível Superior (CAPES – Finance Code 001), Conselho Nacional de Desenvolvimento Científico e Tecnológico (CNPq), Sisfóton-MCTI, Fundação de Amparo à Pesquisa do Estado de São Paulo (FAPESP - 2018/11283-7), the Air Force Office of Scientific Research (FA9550-15-1-0521) and Army Research Laboratory (W911NF-17-1-0123).

References

[1] J. Lv, Y. Cheng, W. Yuan, X. Hao, F. Chen, Three-dimensional femtosecond laser fabrication of waveguide beam splitters in $LiNbO_3$ crystal, Opt. Mater. Express 5 (2015) 1274, https://doi.org/10.1364/ome.5.001274.

[2] A. Abou Khalil, J.P. Bérubé, S. Danto, J.C. Desmoulin, T. Cardinal, Y. Petit, R. Vallée, L. Canioni, Direct laser writing of a new type of waveguides in silver containing glasses, Sci. Rep. 7 (2017), https://doi.org/10.1038/s41598-017-11550-0.

[3] J.M. Maia, V.A. Amorim, D. Viveiros, P.V.S. Marques, Femtosecond laser micromachining of an optofluidics-based monolithic whispering-gallery mode resonator coupled to a suspended waveguide, Sci. Rep. 11 (2021), https://doi.org/10.1038/s41598-021-88682-x.

[4] A. Butkutė, L. Jonušauskas, 3D manufacturing of glass microstructures using femtosecond laser, Micromachines 12 (2021), https://doi.org/10.3390/mi12050499.

[5] Z. Liu, J. Xu, Z. Lin, J. Qi, X. Li, A. Zhang, J. Lin, J. Chen, Z. Fang, Y. Song, W. Chu, Y. Cheng, Fabrication of single-mode circular optofluidic waveguides in fused silica using femtosecond laser microfabrication, Opt Laser. Technol. 141 (2021), https://doi.org/10.1016/j.optlastec.2021.107118.

[6] R. Bai, Y. Gao, C. Lu, J. Tan, F. Xuan, Femtosecond laser micro-fabricated flexible sensor arrays for simultaneous mechanical and thermal stimuli detection, Meas. J. Int. Meas. Confed. 169 (2021), https://doi.org/10.1016/j.measurement.2020.108348.

[7] J.M.P. Almeida, L. De Boni, W. Avansi, C. Ribeiro, E. Longo, A.C. Hernandes, C. R. Mendonca, I. De Física, D.S. Carlos, U.D.S. Paulo, S. Carlos, Generation of copper nanoparticles induced by fs-laser irradiation in borosilicate glass, Opt Express 20 (2012) 15106–15113, https://doi.org/10.1364/OE.20.015106.

[8] K.T. Paula, K.L.C. Silva, A.V.A. Mattos, M.B. de Andrade, R.C. Sanfelice, D. T. Balogh, C.R. Mendonça, Controlling surface wettability in methacrylic copolymer containing azobenzene by fs-laser microstructuring, Opt. Mater. 116 (2021) 111083, https://doi.org/10.1016/J.OPTMAT.2021.111083.

[9] C.R. Mendonca, D.S. Correa, F. Marlow, T. Voss, P. Tayalia, E. Mazur, Three-dimensional fabrication of optically active microstructures containing an electroluminescent polymer, Appl. Phys. Lett. 95 (2009), https://doi.org/10.1063/1.3232207.

[10] S.N.C. Santos, G.F.B. Almeida, J.M.P. Almeida, A.C. Hernandes, C.R. Mendonça, Waveguides fabrication by femtosecond laser in Tb^{3+}/Yb^{3+} doped CaLiBO glasses, Opt Laser. Technol. 140 (2021), https://doi.org/10.1016/j.optlastec.2021.107030.

[11] S. Nakashima, R. Okabe, K. Sugioka, A. Ishida, Fabrication of magneto-optical waveguides inside transparent silica xerogels containing ferrimagnetic Fe_3O_4 nanoparticles, Opt Express 26 (2018) 31898, https://doi.org/10.1364/oe.26.031898.

[12] T. Shih, R.R. Gattass, C.R. Mendonca, E. Mazur, Faraday rotation in femtosecond laser micromachined waveguides, Opt Express 15 (2007) 5809–5814, https://doi.org/10.1364/OE.15.005809.

[13] Y. Li, X. Gao, M. Jiang, Q. Sun, J. Tian, Fabrication of magneto-optical microstructure by femtosecond laser pulses, Chin. Opt Lett. 10 (2012) 102201–102203, https://doi.org/10.3788/col201210.102201.

[14] H. Fang, L. Weinan, B. Jing, Z. Kaiming, L. Xuewen, H. Rongqing, Z. Xiaolin, C. Guanghua, Femtosecond-laser-written waveguide in magneto-optical glass, Acta Opt. Sin. 33 (2013) 1–6, https://doi.org/10.3788/AOS201333.0314002.

[15] Q. Liu, B.F. Johnston, S. Gross, M.J. Withford, M.J. Steel, Investigation of laser processing of magneto-optical glasses, in: Adv. Photonics 2013, Optica Publishing Group, 2013, https://doi.org/10.1364/IPRSN.2013.JT3A.16. JT3A.16.

[16] H. Yin, Y. Gao, Y. Gong, R. Buchanan, J. Song, M. Li, Wavelength dependence of Tb^{3+} doped magneto-optical glass Verdet constant, Ceram. Int. 44 (2018) 10929–10933, https://doi.org/10.1016/j.ceramint.2018.03.156.

[17] H. Yang, Z. Zhu, Magneto-optical glass mixed with Tb^{3+} ions: high Verdet constant and luminescence properties, J. Lumin. 231 (2021), https://doi.org/10.1016/j.jlumin.2020.117804.

[18] Q. Chen, Q. Chen, H. Wang, G. Wang, S. Yin, Magneto optical properties of rare earth Tb_2O_3 doped PbO-Bi_2O_3-B_2O_3 glass, J. Non-Cryst. Solids 470 (2017) 99–107, https://doi.org/10.1016/j.jnoncrysol.2017.05.008.

[19] Z. Chen, X. Wang, J. Wang, Y. Hang, Highly transparent terbium gallium garnet crystal fabricated by the floating zone method for visible – infrared optical isolators, Opt. Mater. 46 (2015) 12–15, https://doi.org/10.1016/j.optmat.2015.03.034.

[20] I. Kriegel, F. Scotognella, Magneto-optical switching in microcavities based on a TGG defect sandwiched between periodic and disordered one-dimensional photonic structures, Optik 142 (2017) 249–255, https://doi.org/10.1016/j.ijleo.2017.05.091.

[21] M. Elisa, L. Boroica, B.A. Sava, S.M. Iordache, A.M. Iordache, I.C. Vasiliu, R. C. Stefan, A.C. Galca, V. Kuncser, M. Eftimie, Synthesis and characterization of a titanium phosphate-tellurite glass for Faraday rotators, J. Am. Ceram. Soc. 103 (2020) 3978–3990, https://doi.org/10.1111/jace.17071.

[22] F. Suzuki, N. Fujita, F. Sato, Small short-wavelength optical isolator using Tb^{3+}-rich magneto-optical glass, in: Proc. SPIE, 2019, p. 37, https://doi.org/10.1117/12.2503595.

[23] H. Furuse, R. Yasuhara, K. Hiraga, S. Zhou, High Verdet constant of Ti-doped terbium aluminum garnet (TAG) ceramics, Opt. Mater. Express 6 (2016) 191, https://doi.org/10.1364/ome.6.000191.

[24] I.A.A. Terra, L.J. Borrero-González, T.R. Figueredo, J.M.P. Almeida, A. C. Hernandes, L.A.O. Nunes, O.L. Malta, Down-conversion process in Tb^{3+}-Yb^{3+} co-doped Calibo glasses, J. Lumin. 132 (2012) 1678–1682, https://doi.org/10.1016/j.jlumin.2012.02.019.

[25] S.N.C. Santos, K.T. Paula, J.M.P. Almeida, A.C. Hernandes, C.R. Mendonça, Effect of Tb^{3+}/Yb^{3+} in the nonlinear refractive spectrum of CaLiBO glasses, J. Non-Cryst. Solids 524 (2019), https://doi.org/10.1016/j.jnoncrysol.2019.119637.

[26] J.M.P. Almeida, P.H.D. Ferreira, D. Manzani, M. Napoli, S.J.L. Ribeiro, C. R. Mendonça, Metallic nanoparticles grown in the core of femtosecond laser micromachined waveguides, J. Appl. Phys. 115 (2014), https://doi.org/10.1063/1.4875485.

[27] R. Osellame, G. Cerullo, R. Ramponi, Femtosecond Laser Micromachining: Photonics and Microfluidic Devices in Transparent Materials, Spinger, 2011, https://doi.org/10.1007/978-3-642-23366-1.

[28] R. Osellame, N. Chiodo, G. Della Valle, S. Taccheo, R. Ramponi, G. Cerullo, A. Killi, U. Morgner, M. Lederer, D. Kopf, Optical waveguide writing with a diode-pumped femtosecond oscillator, Opt Lett. 29 (2004) 1900–1902, https://doi.org/10.1364/OL.29.001900.

[29] D. Body, B.L. Chadwick, Optimization of the spectral data processing in a LIBS simultaneous elemental analysis system, Spectrochim. Acta Part B At. Spectrosc. 56 (2001) 12, https://doi.org/10.1016/S0584-8547(01)00186-0.

[30] J.M. Liu, Simple technique for measurements of pulsed Gaussian-beam spot sizes, Opt Lett. 7 (1982) 196–198, https://doi.org/10.1364/OL.7.000196.

[31] B.E.A. Saleh, M.C. Teich, Fundamentals of Photonics, John Wiley & Sons, Inc., 1991, https://doi.org/10.1002/0471213748.